(T1.4-P8)

Tsunami Waves Generated by Earthquakes: Computed by Means of Numerical Simulations in the Western Black Sea

Lyuba Dimova [1], Alberto Armigliato [2], Gianluca Pagnoni [2], Filippo Zaniboni [2], Stefano Tinti [2], Reneta Raykova [1]
[1] Department of Meteorology and Geophysics, Faculty of Physics, Sofia University “St. Kl. Ohridski”, Bulgaria (lyuba_dimova@phys.uni-sofia.bg)
[2] Sector Geophysics, Department of Physics and Astronomy, University of Bologna, Italy

CTBT: SCIENCE AND TECHNOLOGY 2017 CONFERENCE

Abstract

In this work we present numerical simulations of tsunami waves generated by earthquakes in the region of the western Black Sea. We take into account three main seismic sources (two of them placed near the northern coast of Bulgaria and one near the northwestern Turkish Black Sea coast). The propagation of the tsunami waves is simulated through the numerical code UBO-TSUFD. The tsunami is computed on three different grids – one for the whole area of the Black Sea (resolution 500 m), and two smaller grids (resolution 50 m and 250 m) placed near the northern Bulgarian coast (Cape Kaliakra-Kavarna-Varna). The geometric parameters of the seismic sources are estimated. The distribution of maximum water elevation, maximum water column on land and maximum particle velocity fields are calculated and presented. The impact on the coast is evaluated trough the synthetic marigrams chosen for these simulations.

Seismic Sources – Tsunami Initial Conditions

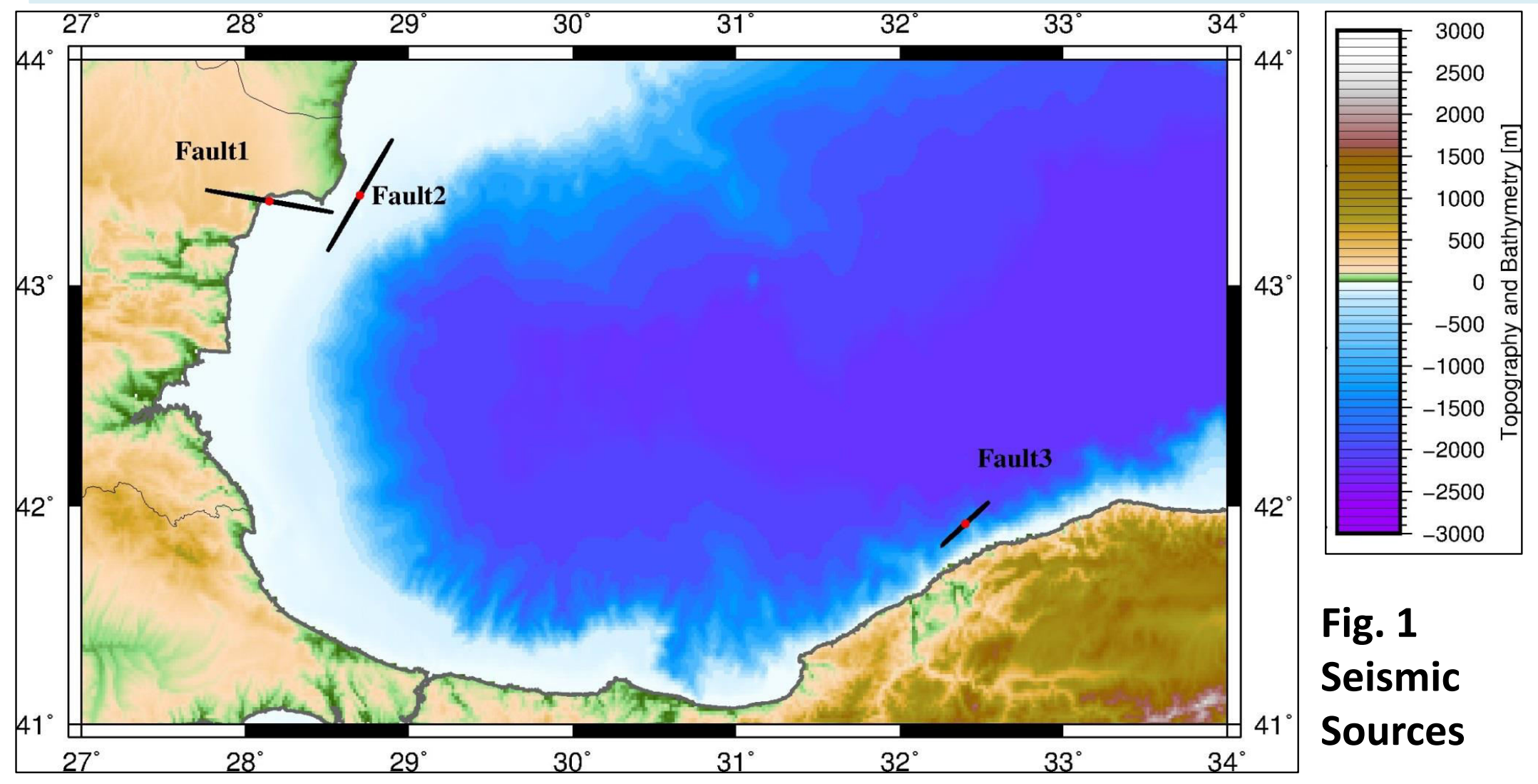

Fig. 1 Seismic Sources

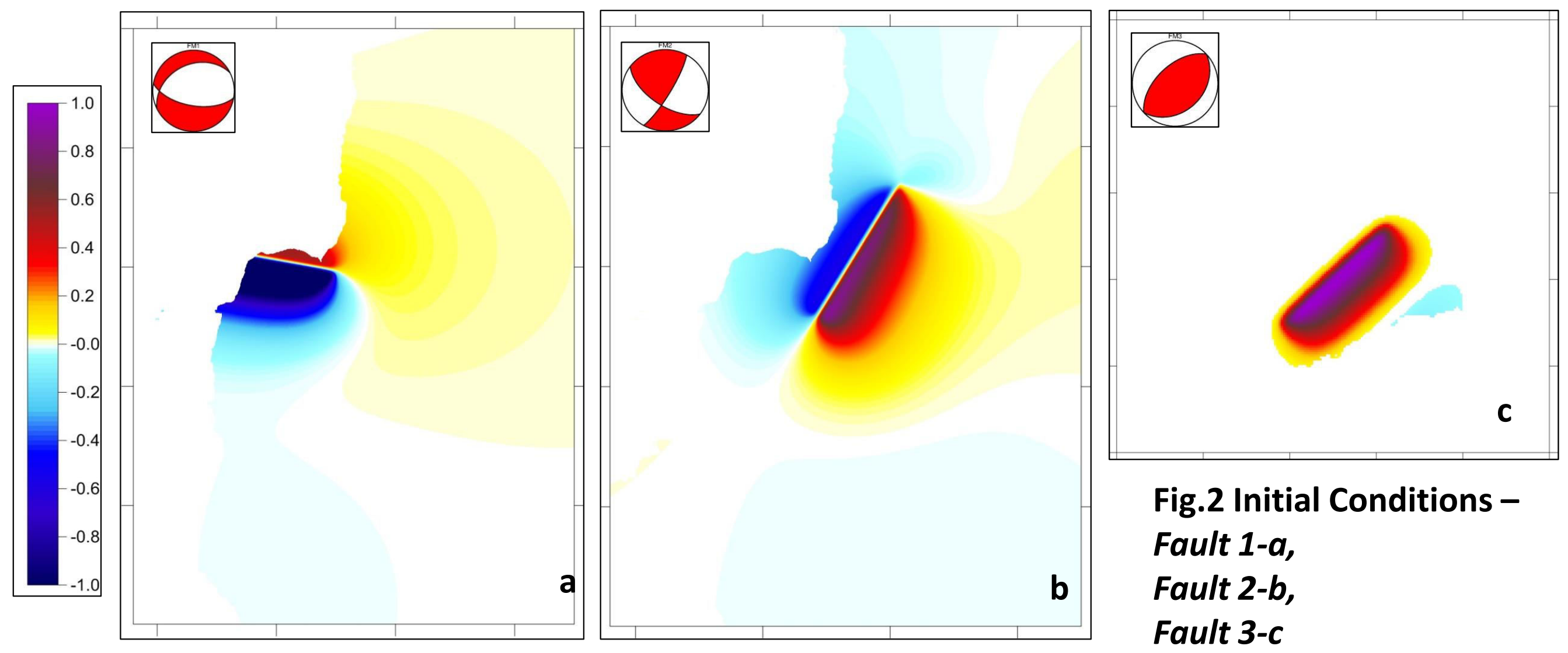

Fig.2 Initial Conditions – ***Fault 1-a, Fault 2-b, Fault 3-c***

Table 1

	Fault 1	Fault 2	Fault 3
L (km)	64	64	32.5
W (km)	29	29	17
Slip (m)	3.5	3.5	2.0
Strike (°)	100	30	47
Dip (°)	60	80	34
Rake (°)	290	150	90
Mw	7.5	7.5	7.0
Upper Border Depth (m)	2000	2000	3000
Upper Border Middle Point (UTM35T)	(593000.00, 4803000.00)	(637663.13, 4806639.11)	(947846.56, 4655015.76)

By means of the fault database compiled in SHARE - *The European Database of Seismogenic Faults*, tsunamigenic zones in the area of western Black Sea are taken into account (Fig. 1). Fault 1 and Fault 2 are associated with events characterized by tsunami intensity 5 of 6 *(Sieberg-Ambraseys* scale). The geometry of the faults (Table 1) is calculated by the regressions proposed by *Mai and Beroza (2000)* and *Wells and Coppersmith (1994).* The coordinates of the Upper Border Middle Point of the faults are converted from the geographical to the Universal Transverse Mercator coordinate system. Focal mechanism solutions are in accordance with recent earthquakes and the geological settings in the region. Initial conditions shown in Fig. 2 are calculated by means of *Okada`s formulas (1992)* that result from the analytical integration of the double-couple point-source solutions over a rectangle of length L and width W. In Table 2 we summarize the properties of grids used in these simulations. Topography and bathymetry data are taken from GEBCO, EMODNET and ALOS.

Computational Grids and Propagation of Tsunami

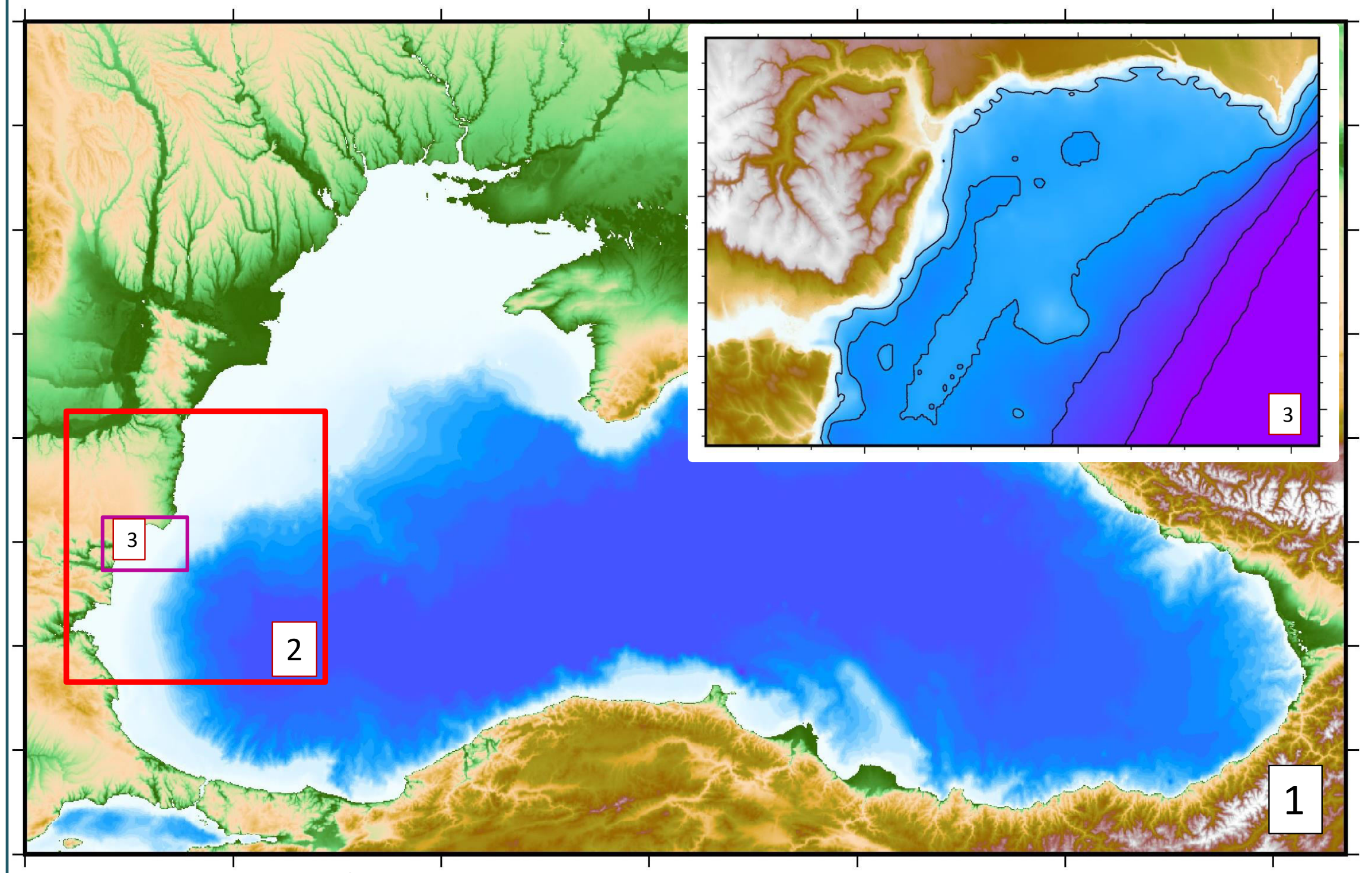

Fig.3 Computational Grids

Table 2

Grid	Resolution (m)	Nodes	Rows	Columns	Time step (s)
1	500	4068141	2541	1601	1
2	250	742742	835	1127	0.5
3	50	881666	1151	766	0.5

Fig 4. Phase Velocity

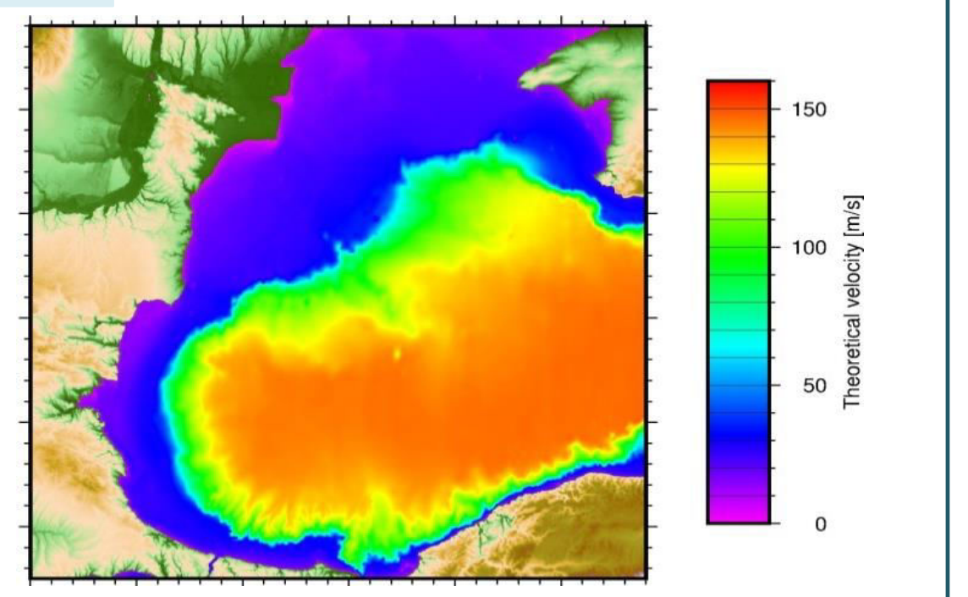

The phase velocity of tsunami waves according to the long-wave theory is given by the expression $c = \sqrt{gh}$, where h is the depth, and g the gravity acceleration and is plotted in Fig 4. The speed is larger than 150 m s^{-1} far from the shore while in the nearshore region it decreases considerably. The theory for tsunami propagation is based on two conservation laws, in case of no energy dissipation, namely the mass conservation (continuity equation) and the momentum conservation, and on appropriate boundary conditions. Tsunami simulations are performed by solving Navier-Stocks equations in the shallow-water theory approximation by using the finite differences technique. An explicit leap-frog scheme on a staggered grid is used in the calculations. Propagation of tsunami waves from the *Fault 3* is presented in Fig. 5. *Fault 3* is associated with the geological setting of the south-western depression in the Black Sea. The most recent observed tsunami due to an earthquake in this region was in 1968 and affected Amasra and Fatsa. The estimated magnitude of the earthquake was 6.8.

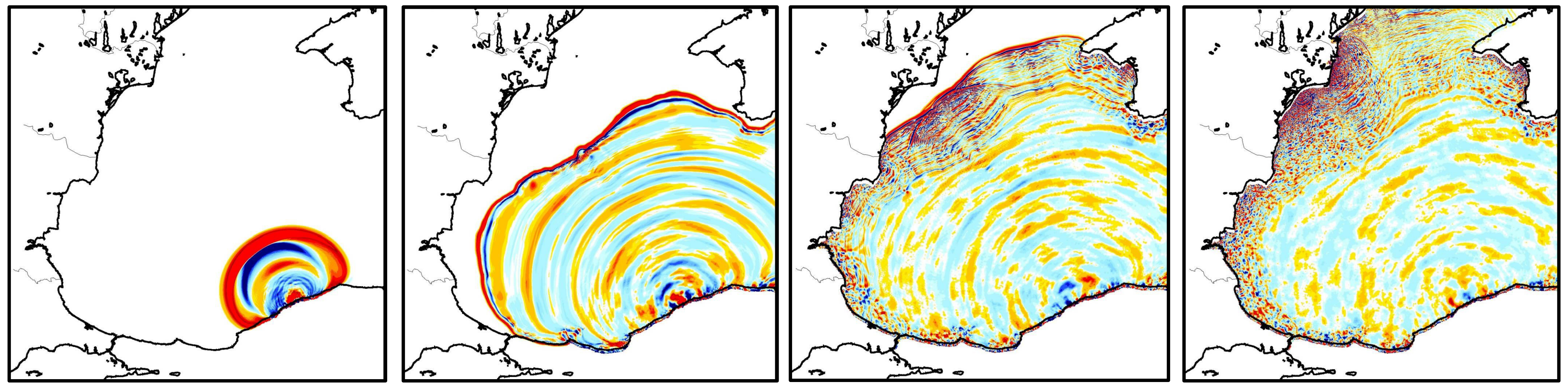

Fig.5 Snapshots of the propagation

Snapshots taken at 10min, 40min, 100min and 120min after the origin time. The first positive wave can be seen clearly. In the north west, the effect of shoaling induced by the decreasing of the phase velocity of the waves approaching the shore can be seen clearly in the simulations.

Tsunami impact on the coast

Fig. 6 Maximum Water Elevation (a1, a2), Maximum Water Column on land (b1, b2) and Maximum Particle Velocity (c1, c2)

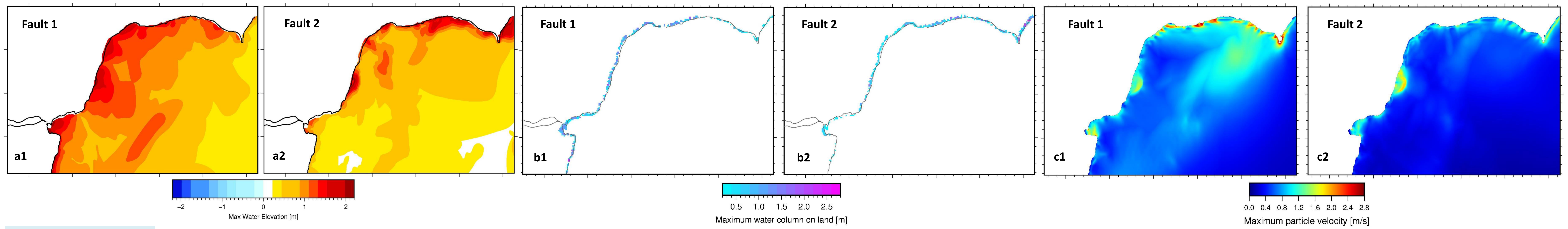

Fig.7 Position of selected synthetic marigrams

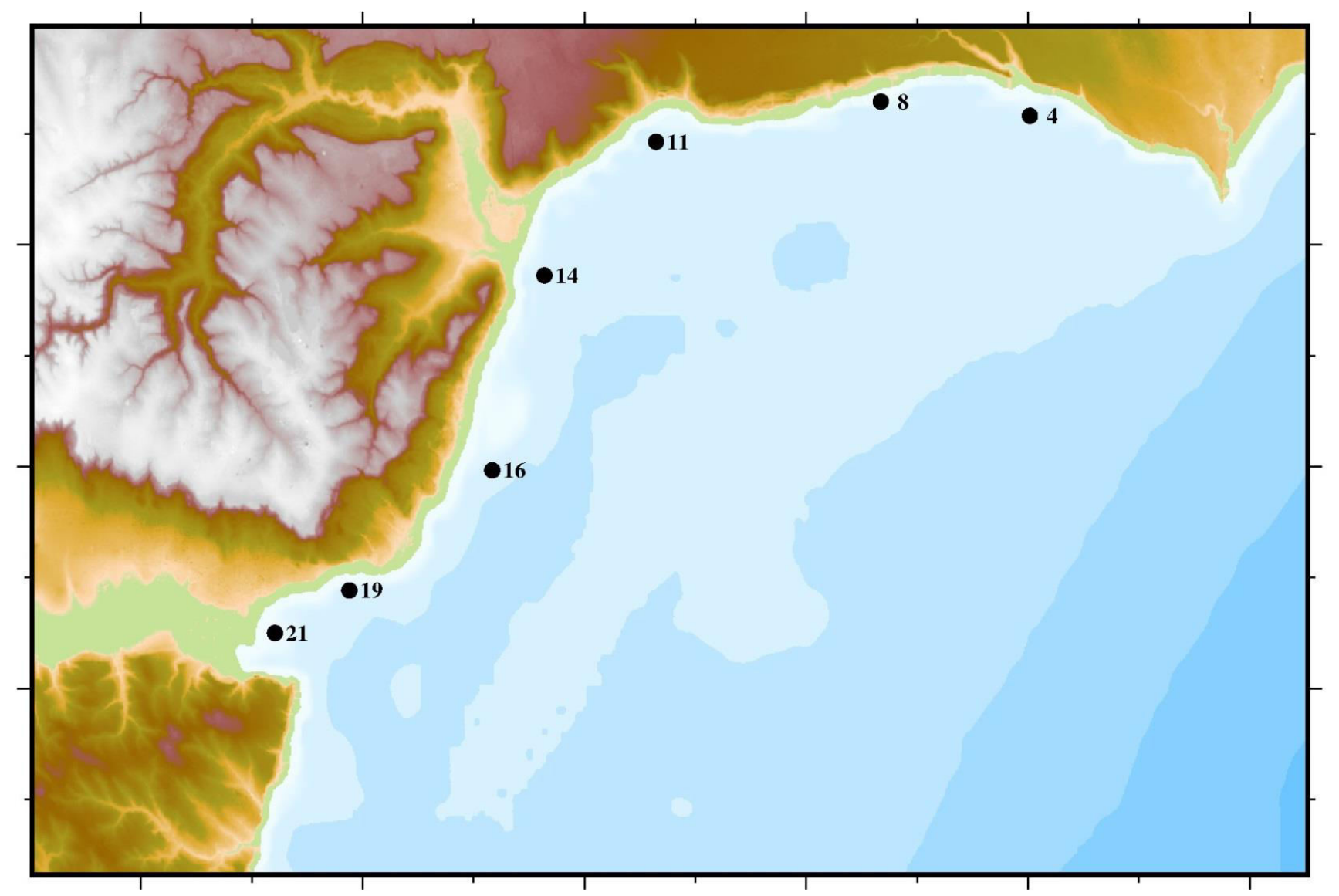

Table 3

№	Lat (°)	Lon (°)	Easting (m)	Northing (m)	Region
4	43.3969	28.37167	611081	4805812.74	Kavarna
8	43.4037	28.28879	604358	4806454.48	Topola
11	43.3887	28.16343	594230	4804641.28	Balchik
14	43.3351	28.10033	589198	4798619.71	Albena
16	43.2563	28.06991	586844	4789836.63	Golden Sands
19	43.2082	27.98974	580400	4784417.29	Varna
21	43.1913	27.94817	577044	4782500.71	Varna

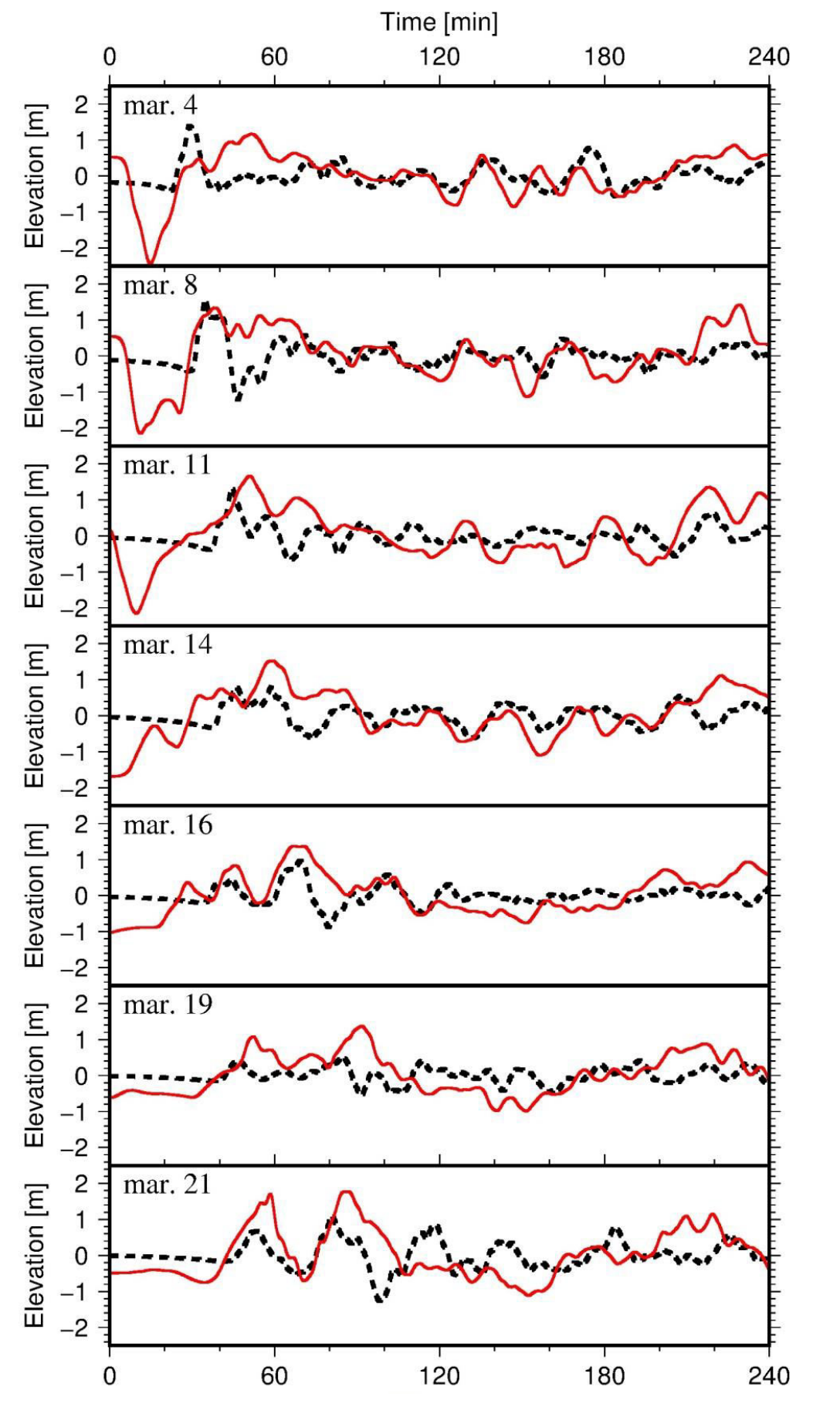

Fig.8 Computed time series for ***Fault 1*** **and** ***Fault 2*** **for the first 240 min of tsunami propagation**

References

Guidoboni, E., A. Comastri, G. Traina, Catalogue of Ancient Earthquakes in the Mediterranean Area up to the 10th Century, 1, SGA, 1994.
Mai, P.M., G.C. Beroza, Source scaling properties from finite-fault-rupture models, Bulletin of Seismological Society of America, 90, 3, 2000.
Maramai, A., B. Brizuela, L. Graziani, The Euro-Mediterranean Tsunami Catalogue, Annals of Geophysics, 57, 4, 2014.
Okada, Y., Internal deformation due to shear and tensile faults in a half space, Bulletin of Seismological Society of America, 82, 2, 1992.
Papadopoulos, G. A., E. Gràcia, R. Urgeles, V. Sallares, P. M. De Martini, D. Pantosti, M. González, A. Yalciner, J. Mascle, D. Sakellariou, A. Salamon, S. Tinti, V. Karastathis, A. Fokaefs, A. Camerlenghi, T. Novikova, A. Papageorgiou, Historical and pre-historical tsunamis in the Mediterranean and its connected seas: Geological signatures, generation mechanisms and coastal impacts, Marine Geology, 2014, 354.
Tinti, S., R. Tonini, The UBO-TSUFD tsunami inundation model: validation and application to a tsunami case study focused on the city of Catania, Italy, Natural Hazards and Earth System Sciences, 13, 1759, 2013.
Wells, D., K. Coppersmith, Empirical relationship among magnitude, rupture length, rupture width, rupture area and surface displacement, Bulletin of Seismological Society of America, 84, 4, 1994.

Acknowledgments

I, the first author, would like to thank the Tsunami Research Team of the University of Bologna for the opportunity to work with them. The presented poster is supported by project 80-10-21/19.04.2017 “Numerical modelling of tsunami waves in the region of Aegean Sea” funded by Sofia University and Bulgarian Ministry of Education and Science.